Description of the IRAS 9P/Tempel 1 Datasets, including Photometry

C.M. Lisse, University of Maryland

2003-10-15

I Introduction

Comet 9P/Tempel 1 was observed and detected by only one of the several highly sensitive IR cryogenic telescope spacecraft to date - IRAS. Long wavelength infrared observations of a comet are necessary in order to detect and characterize the nucleus and dust of a comet. To make an assessment of the dust hazard presented by large, massive coma dust particles to the Deep Impact spacecraft during its rendezvous and impact with the comet, we have thus analyzed archival 1983 IRAS data for 9P/Tempel 1, updated for new instrument calibrations and improved extraction of extended sources. The scientific results of this analysis will be published in the literature as the paper "The Coma of Comet 9P/Tempel 1" by Lisse et al. (2005).

The datasets described below began as IRAS observations of 9P/Tempel 1 archived at the Infrared Processing and Analysis Center (IPAC), which were then corrected for the effects of extended source emission by Russell Walker. He converted the reconstructed images into FITS files and delivered the images to the Deep Impact project in 2000 and 2001. The details of the work done by Walker have been described in the explanatory supplements provided with the reconstructed FITS files; for more information on this step of the analysis, we refer the reader to these documents (Walker 2000 and 2001). There the reconstructed images were unpacked, stripped of any extraneous backgrounds, and re-calibrated to the latest IRAS absolute calibration, before being delivered to the PDS for archiving. The details of these last steps are described below.

II Instrumental

As NASA's first orbiting cryogenic IR telescope, the US-UK-Netherlands IRAS mission (Neugebauer 1984), of duration 300 days in 1983, broke new ground in the study of the infrared sky. Without terrestrial atmospheric emission and with a telescope at liquid helium temperatures, the instrumental backgrounds were extremely low. The photoconductive solid-state detectors were also novel for the time; previously used ground-based detectors had consisted of heat sensing composite bolometers or single element photoconductive sensors (Young 1982, Reike et al. 1986). Unlike today's IR focal plane arrays, the IRAS focal plane consisted of three different kinds of single element detectors staggered in position throughout the focal plane. Typical instantaneous fields of view of the detectors varied from 0.76 arcminutes by 4.45 arcminutes at 12 micron to 3.03 arcminutes by 5.05 arcminutes at 100 micron. "Imaging" the sky consisted of collecting the time-ordered data streams from each detector element, mapping the element FOV onto the sky, and coadding the resulting skymaps from the different detector elements. The IRAS instrument suite also included a low-resolution spectrometer, the LRS, with resolving power R of about 20 to 60 over the wavelength range 7.7 to 22.6 micron (Raimond et al. 1985, Olnon and Raimond 1986).

III Data

The IRAS data products typically used for scientific analysis consist of the Faint Source Catalogue, Point Source Catalogue, and IRAS Sky Survey Atlas (ISSA) skymaps archived at IPAC. The IRAS Explanatory Supplement (Beichman et al. 1988) describes the data in detail and is available online at http://www.ipac.caltech.edu.

Photometry of comets suffers in the point source catalogs due to the finite spatial filters used to detect point sources in the time ordered data stream, and due to the motion of comets in the ISSA images. Walker made improvements on extracting the wings of faint extended emission directly from the IRAS time-ordered data stream, using an extraction

algorithm moving in a comet-centric coordinate system to re-create comet maps down to the limiting sensitivity of the IRAS instrument. Refer to the Explanatory Supplements for the IRAS Additional (Pointed) Observations and Survey Scans for 9P/Tempel 1 (Walker 2000 and 2001).

Survey Mode Data

The bulk of the IRAS observation time was spent in "survey mode", where the sky was systematically mapped with a series of overlapping and confirming scans. The sampling redundancy can be used to produce a time-averaged sky survey with limiting magnitude fainter than the instantaneous sensitivity, such as the IRAS Faint Source Survey, or to improve the spatial resolution in the scanned fields. The survey images were filled using the following algorithm: 1. The width (delta elongation) of the image was determined essentially by the width of the focal plane array, thus both right and left sides are filled at the same time. 2. In all cases the scan was by rotation (inclination) about the Earth-Sun line (plus or minus 30 deg). 3. In the case of the survey images the scans were always in a clockwise direction about the Earth-Sun line. The data were then spatially coadded for several survey scans without regard to the sequence of data taking.

Construction of extended source images from survey data is complicated by the fact that the confirming scans cross each other at varying angles. Construction of extended solar system object images also requires compensation for the motion of the object and the changing spacecraft parallax during the relatively large time interval (greater than 103 minutes) between the confirming scans necessary to build the image. Details of the survey mode image processing and recalibration analysis are given by Cohen et al. in "Spectral Irradiance Calibration in the Infrared, I. Ground-based and IRAS Broadband Calibrations" (1992) and in the Explanatory Supplement for the IRAS Survey Scans for 9P/Tempel 1 (Walker 2000).

Walker reconstructed Survey images and supplied the images to the Deep Impact project as FITS files. He obtained in-band photometry the reconstructed FITS images, after applying an additional background removal, and delivered these data to the Deep Impact

project (Walker 2000). It was found that the aperture photometry curves for comet 9P/Tempel 1 did not converge to an asymptote at aperture sizes much larger than the coma width without this step. Therefore, Lisse used an improved method to produce new aperture photometry to replace data supplied by Walker. Lisse used a background removal algorithm that employed a 2-D quadratic surface fit to a synthetic background, created by taking the original in-band radiance image produced by Walker and replacing all pixels in a 25 pixel radius centered at the nucleus with the median value of the image. The masked region size was chosen to eliminate any contamination of the background by cometary emission. The surface fit was then subtracted from the original image. Multi-aperture photometry was extracted for each resulting image. One table of aperture photometry results was produced for each image. Table 1 provides an example of the set of results for one Survey Scan image.

Table 1. 100-micron Aperture Photometry of 9P/Tempel 1, generated by Lisse from the reconstructed AO image, S421_100UM_29_RADIANCE.FIT, produced by Walker.

-Aperture Radius- (pix,24 arcsec pixels)	(arcsec)	In-band Signal Inside Aperture Radius (W/cm2/sr)	Background Subtracted (W/cm2/sr)	Statistical Noise on Signal Inside Aperture (W/cm2/sr)
0	0	0.00000E+00	0.00000E+00	0.00000E+00
1	24	2.03791E-11	1.25456E-11	2.14629E-12
2	48	9.00316E-11	6.26063E-11	4.79924E-12
3	72	2.10228E-10	1.62505E-10	7.73854E-12
4	96	3.34128E-10	2.87034E-10	1.02932E-11
5	120	4.79302E-10	4.85413E-10	1.34036E-11
6	144	5.84369E-10	6.82849E-10	1.59173E-11
7	168	6.67905E-10	9.09265E-10	1.84006E-11
8	192	7.48235E-10	1.23362E-09	2.14629E-11
9	216	8.13224E-10	1.54154E-09	2.40442E-11
10	240	8.90442E-10	1.91796E-09	2.68929E-11
11	264	9.91629E-10	2.27855E-09	2.93892E-11
12	288	1.15366E-09	2.71931E-09	3.21943E-11
13	312	1.36161E-09	3.19990E-09	3.50377E-11
14	336	1.58428E-09	3.63887E-09	3.74833E-11
15	360	1.88490E-09	4.17896E-09	4.03250E-11
16	384	2.17160E-09	4.68463E-09	4.28452E-11
17	408	2.45827E-09	5.29015E-09	4.57567E-11
18	432	2.68620E-09	5.87209E-09	4.84224E-11
19	456	2.84864E-09	6.47716E-09	5.10843E-11
20	480	2.95317E-09	7.10325E-09	5.37858E-11
21	504	2.99231E-09	7.71504E-09	5.63374E-11
22	528	2.99847E-09	8.41537E-09	5.92079E-11
23	552	2.99238E-09	9.08132E-09	6.18711E-11
24	576	2.97853E-09	9.74613E-09	6.44958E-11

One can derive calibrated absolute photometry using the in-band radiances found in the aperture photometry tables produced by Lisse. First, convert the derived in-band radiances (Watts/cm^2/sr) to flux density units (Jy/sr) by dividing the in-band radiance by (13.48, 5.16, 2.58, and 1.00) x 10^{-18} for the 12, 25, 60, and 100 micron bands, respectively. A "color correction" must then be applied to allow for the shape of the spectrum through the IRAS bandpass. For example, given a greybody at 250K, similar to the emission detected by IRAS from Tempel 1 near perihelion in 1983, the flux densities should be divided by 0.87, 1.11, 1.19, and 1.07 for the 12, 25, 60, and 100 micron bands, respectively. Finally, the COBE/IRAS recalibration factors of 1.0, 1.0, 0.87, and 0.72 must be divided into each band's photometry in order to correct the original IRAS calibration with respect to the ecliptic poles to the COBE/DIRBE calibration with respect to its more accurate internal on-board 2.4 K blackbody. Figure 2 presents the results of this calculation in units of $\nu * I_\nu$ (Jy/sr) * Ω for a beam with a radius 90 arcseconds where ν is the frequency and Ω is the area of the beam.

The application of the COBE/DIRBE recalibration to the IRAS data for Tempel 1 is controversial, because the effective scan rate across the moderately extended Tempel 1 nucleus and coma is not easily determined, and the recalibration depends on the frequency-dependent gain calibration of the early-generation IRAS focal plane detectors. However, the spectral energy distribution (SED) described by the extracted photometry of Walker, without the correction, is unlike any SED ever measured for cometary dust. Therefore, we present the background information on the recalibration and our suggestions for its use in the Appendix. We leave it up to the user to decide if the COBE/DIRBE re-calibration factors should be applied.

Additional Observations

There are more detections of Tempel 1 in the IRAS database than were produced in the all-sky survey. IRAS devoted almost 40% of its observing time to Additional Observations (AOs), that is, pointed observations of selected fields of interest; these were carried out during an IRAS "Satellite Operating Plan" (SOP).

The AOs scans were rasters, that is, clockwise and counter-clockwise alternating. The data were spatially coadded to produce the images with no regard for the sequence of radiance measurements. Details of the AO image processing and recalibration analysis are given in Cohen et al. in "Spectral Irradiance Calibration in the Infrared, I. Ground-based and IRAS Broadband Calibrations" (1992) and in Explanatory Supplement for the IRAS Additional Observations of 9P/Tempel 1 (Walker 2001). Note that while construction of comet images from Survey scans requires compensation for comet and spacecraft motion during the large time interval (about 6000 seconds) between scans, the duration of an AO is usually less than 800 seconds. Motion compensation is not necessary if the comet's apparent motion is sufficiently small. In all the Tempel 1 Additional Observations, the apparent motion of the comet is much smaller than the 15 arcsec default pixel size used. The AO's were completed in 0.14 of an IRAS orbit, producing a maximum of 1.1 arcsec parallax for a comet at a distance of 1 AU.

In-band photometry was obtained by Lisse from the resulting images in the same manner as for the survey observations. The IRAS AO images reanalyzed by the image construction techniques of Walker with 20 iterations were subjected to an additional background removal step. The background was found for each image by replacing all data in a 25-pixel radius area centered at the nucleus with its median pixel value, and then surface fitting the resulting image. The surface fit was then subtracted from the original image. Multi-aperture photometry was extracted for each resulting image. One table of aperture photometry results was generated for each image. Table 2 provides an example of the set of results for one AO image.

Table 2. 12-micron Aperture Photometry of 9P/Tempel 1, generated by Lisse from the reconstructed AO image, S287_O13_12UM_20_RADIANCE.FIT, produced by Walker.

-Aperture Radius-- (pix,15 arcsec pixels)	(arcsec)	In-band Signal Inside Aperture Radius ($W/cm^2/sr$)	Background Subtracted ($W/cm^2/sr$)	Statistical Noise on Signal Inside Aperture ($W/cm^2/sr$)
0	0	0.00000e+00	0.00000e+00	0.00000e+00
1	15	2.86259e-09	2.19968e-12	4.88455e-12
2	30	1.51226e-08	1.09939e-11	1.09222e-11
3	45	3.27767e-08	2.85706e-11	1.76115e-11
4	60	4.71766e-08	5.05223e-11	2.34255e-11
5	75	6.05386e-08	8.55964e-11	3.05040e-11
6	90	6.76834e-08	1.20617e-10	3.62248e-11
7	105	7.31972e-08	1.61212e-10	4.18763e-11
8	120	7.84333e-08	2.18534e-10	4.88455e-11
9	135	8.28309e-08	2.74079e-10	5.47200e-11
10	150	8.71235e-08	3.42546e-10	6.12032e-11
11	165	9.11944e-08	4.08705e-10	6.68844e-11
12	180	9.53380e-08	4.89397e-10	7.32682e-11
13	195	9.88041e-08	5.78099e-10	7.97394e-11
14	210	1.01196e-07	6.61924e-10	8.53748e-11
15	225	1.03213e-07	7.62621e-10	9.17723e-11
16	240	1.04598e-07	8.58630e-10	9.75076e-11
17	255	1.05837e-07	9.77613e-10	1.04134e-10
18	270	1.06894e-07	1.09097e-09	1.10200e-10
19	285	1.07846e-07	1.21034e-09	1.16258e-10
20	300	1.08727e-07	1.33864e-09	1.22406e-10
21	315	1.09608e-07	1.46484e-09	1.28260e-10
22	330	1.10355e-07	1.61111e-09	1.34746e-10
23	345	1.10906e-07	1.75208e-09	1.40807e-10
24	360	1.11261e-07	1.89625e-09	1.46780e-10

One can derive calibrated photometry using the in-band radiances found in the aperture photometry tables produced by Lisse. First, convert the derived in-band radiances ($Watts/cm^2/sr$) to flux density units (Jy/sr) by dividing the in-band radiance by (13.48, 5.16, 2.58, and 1.00) x 10^{-18} for the 12, 25, 60, and 100 micron bands, respectively. A "color correction" must then applied to allow for the shape of the spectrum through the IRAS bandpass. For example, given a greybody at 250K, similar to the emission detected by IRAS from Tempel 1 near perihelion in 1983, the flux densities would be divided by 0.87, 1.11, 1.19, and 1.07 for the 12, 25, 60, and 100 micron bands, respectively. Finally, the COBE/IRAS recalibration factors of 1.0, 1.0, 0.87, and 0.72 must be divided into each band's photometry in order to correct the original IRAS calibration with respect to the ecliptic poles to the COBE/DIRBE calibration with respect to its more accurate internal on-board 2.4 K blackbody.

IV Results of the IRAS 9P/Tempel 1 Observations

Morphology

Sample IRAS comet images are shown in Figure 1. The SNR versus the background is generally highest at 12 micron, at smallest heliocentric distance (r_{comet}) and at smallest geocentric distance (δ).

For the best survey images, the shape of the comet's coma and tail is only slightly larger than that of a point source, with little extension along the Sun-comet vector as would be expected for small dust particles in the coma accelerated by solar radiation pressure (Lisse et al. 1998). Instead, a faint trail of emission, due to large dust particles for which radiation pressure is negligible and with orbital paths very close to the comet nucleus, is seen. The trail radiance is only a few percent of the central condensation radiance, fainter than most detected trails (Sykes et al. 1992), but with an estimated mass greater than 4 x 10^9 kg, assuming a radius greater than 1 mm particles in the trail, as found for 10P/Tempel 2 using IRAS (Sykes, Lien, and Walker, 1990).

For the best AO images, obtained around perihelion, the comet's coma and tail are spatially resolved. The direction of the trail and tail are as expected for particles acting under the influence of solar radiation pressure and gravity. The trail radiance is approximately 10% of the central condensation radiance at the brightness centroid, decreasing to about 0.005 times the peak brightness at distance of 200,000 km from the nucleus. The width of the trail is on the order of 30,000 km at 200,000 km.

Photometry

The IRAS spectrophotometry of comet 9P/Tempel 1 obtained in the 4 broad bandpasses and the LRS in July and August 1983 has been used to determine the nature of the dust emitted by the comet. Using the imaging photometry, Walker et al. (1984, 1986 a,b) reported the comet's dust coma to consist of material with T_{col}/T_{bb} of approximately 1.03, indicative of large, cold, non-absorbing coma dust particles. From the LRS spectrum, Lynch et al. (1995) found a dust of color temperature 230 to 240K at r_{comet} of 1.49 to 1.55 AU, no evidence for a silicate emission feature above the noise, and a dust emission rate Q_{dust} greater than 260 kg/s (assuming all dust to be emitted as greater than 30 micron solid silicate spherical particles of density 2.5 g/cm^3, with the minimum particle size given by the upper limits on any possible silicate emission feature).

Since these publications, significant improvements have been made to the IRAS photometric calibration and to the extraction of faint extended sources from the IRAS time-ordered data stream. Most importantly for this work, the Cosmic Background Explorer (COBE) mission of 1989 - 1990 reflew the 4 IRAS bandpasses with improved understanding of the detector calibration and instrumental zero points. As a result, the IRAS photometric gains were readjusted by 10 - 30% (see Appendix A), with the largest changes occurring in the 60 and 100 micron bandpasses. The effect of these gain changes is to decrease the long wavelength fluxes relative to the short wavelength fluxes, thus increasing the effective color temperature by 20 - 30K (Figure 2) and causing the entire corrected SED to lie very close to that of a greybody in LTE.

Figures

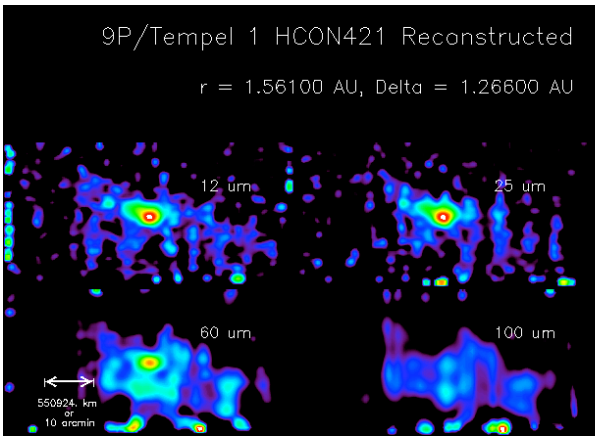

Figure 1a

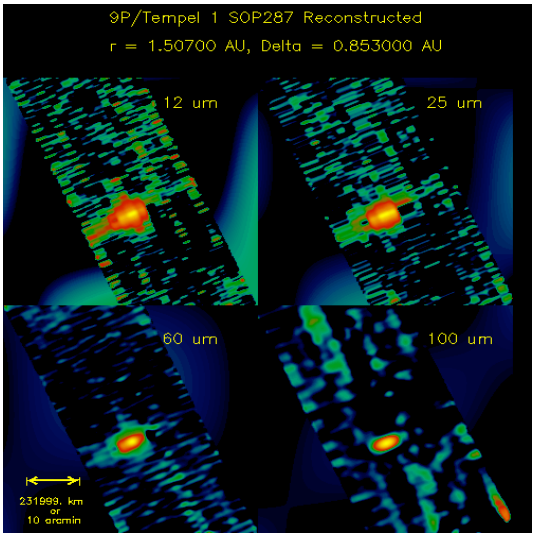

Figure 1b

Figure 1a. IRAS Survey imaging of 9P/Tempel 1 at 12, 25, 60, and 100 microns on 28 July 1983. These 12, 25, 60, and – 100 micron reconstructed survey images with 24 arcsec/pixel resolution show a faint trail, which has increased in brightness relative to the nucleus as the comet retreats from the Earth. South is to the top and West is to the left. The comet is moving towards the lower right, and the projected direction to the Sun is to the lower right. The comet nucleus is the bright point in the center, and the comet trail extends mainly north and west in the anti-velocity direction, i.e. along the orbital path the comet has recently traveled. The projected direction to the Sun is towards the lower right of the image. The trail is brightest in the anti-sunward direction. Images are displayed with the fastest varying axis (x or line samples) increasing to the right and slowest varying axis (y or lines) to the top.

Figure 1b. IRAS in AO mode, images of 9P/Tmpel 1 at 12, 25, 60, and 100 microns on 28 July 1983. These reconstructed AO images with 15 arcsec/pixel resolution best show the comet's trail, which is resolved over the small spatial extent it was observed. The coordinate system is rotated 45 degrees from that of Fig 1(a). East is to the left and North is up. The projected direction to the Sun is towards the upper left of the image at position angle 305 deg. The trail of the comet is spatially resolved in these images, with width 4 to 8 pixels FWHM. The image FOV is 1 deg. Images are displayed with the fastest varying axis (x or line samples) increasing to the right and slowest varying axis (y or lines) to the top.

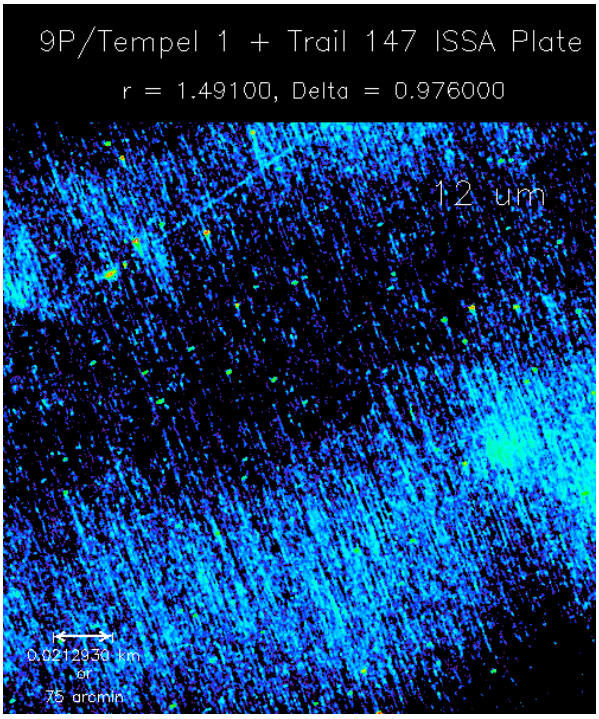

Figure 1c

Figure 1c. IRAS large scale imaging of 9P/Tempel 1 and environs on 11 - 13 July 1983. This is a 12 micron image taken over a number of orbits. The comet nucleus is the bright point in the upper left, and the comet trail extends mainly north and west in the anti-velocity direction, i.e. along the orbital path the comet has recently traveled. The pixel scale is 3 arcmin/pixel. The coordinate system is the same as in Figure 1b. The source of this image is the IRAS Sky Survey Atlas (ISSA) Reject Set.

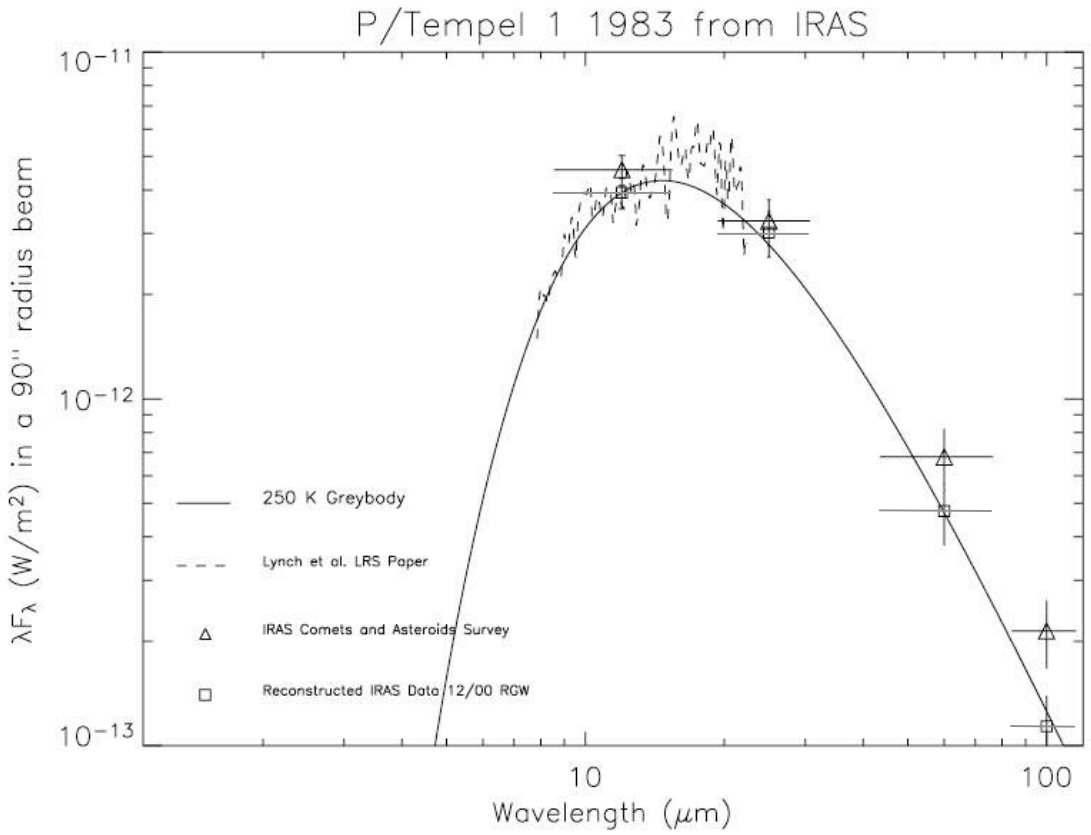

Figure 2. SED for 9P/Tempel 1 derived from IRAS observations near perigee on 12 July 1983. Boxes - Recalibrated IRAS broad band fluxes. These fluxes were calculated by applying the COBE/DIRBE recalibration to the Survey Scan photometry derived by Lisse. The recalibrated fluxes are consistent with a greybody out to 100 micron. The horizontal bars show the FWHM of the bandpass. **Solid curve -** Modified greybody fit to the Tempel 1 IRAS data, with T = 245 +/- 10K, $\varepsilon = \varepsilon_0(\lambda(\mu m)/1\ \mu m)^{-0.00}$ and $\varepsilon_o = 1.5 +/- 0.4 \times 10^{-7}$. There is no evidence of a silicate emission feature or long wavelength emissivity falloff as seen for other comets where the exponent of ε would be less than zero. This is evidence for an abundance of large (radius > 50 microns) dust particles. Triangles - For comparison, fluxes from the 1986 IRAS Asteroid and Comet Survey. Note that the color temperatures estimated from the older data would tend to be 20 - 30K colder than for the recalibrated data. The horizontal bars show the FWHM of the bandpass. Broken lines - IRAS LRS data. The change in noise at 10 – 11 micron is due to the overlap between the two gratings comprising the LRS. Within the errors of the measurements, no silicate emission feature is apparent.

V Appendix

Applicability of the COBE/IRAS Recalibration to the Tempel 1 IRAS Data Extracted by R. Walker (2000, 2001) for the Deep Impact Project

C.M. Lisse, University of Maryland

2003-11-24

The following are 3 references pertinent to the DIRBE/IRAS calibration. A discussion explaining the topic in detail is included after the references.

Reference 1

From http://www.ipac.caltech.edu/ipac/newsletters/oct93/cobe.html:

Comparison of Released COBE Data to IRAS Data (IRAS project note)
By Charles Beichman and Sherry Wheelock

The first data from the DIRBE and FIRAS instruments on the COBE mission have been released by the NSSDC. The data for galactic latitudes within 10 degrees of the plane will provide a wealth of information on the distribution of stars and interstellar material within the galaxy. DIRBE offers information in a 0.7 degree beam for wavelengths from 1-240 micron, while FIRAS offers spectral data in a 7 degree beam. Interested users can contact the NSSDC for instructions on how to pickup the data by anonymous ftp.

Since the IRAS mission was primarily designed to measure point sources and DIRBE was primarily designed to measure extended emission, we believe the COBE/DIRBE calibration is valid and the DIRBE results provide a check on the large-scale performance of IRAS. The COBE/DIRBE Explanatory Supplement (version 19 July 1993) presents a preliminary linear transformation between IRAS and DIRBE data and is presented in the table below. This linear transformation was derived based on carefully selected DIRBE data compared to IRAS scan data. The transformations are applicable to small scales on

the order of an IRAS scan but there is no certainty as to their applicability at smaller spatial scales down to 0.7 degree. The IRAS point source calibration is not affected by these numbers.

The offset term is relevant to the total intensity IRAS product, the IRAS Zodiacal History File (ZOHF). It is not applicable to the IRAS Sky Survey Atlas (ISSA) images since the zodiacal emission was subtracted. The gain term is applicable to both the ISSA and the ZOHF and shows the IRAS measurements at 60 and 100~ micron were too bright relative to DIRBE at large spatial scales. There is no simple prescription for unraveling the varying spatial response of the detectors to effect a more accurate calibration for the ISSA images. The data given in the table below, serve, however, to bound the problem to being no worse than a 28% effect at 100 micron, 13% at 60 micron, and 12% in a 60/100 micron color.

IRAS-DIRBE Transformation [*]

Wavelength	Gain	Offset (MJy/sr)
12 micron	1.06 +/- 0.02	-0.48 +/- 0.43
25 micron	1.01 +/- 0.02	-1.32 +/- 0.74
60 micron	0.87 +/- 0.05	+0.13 +/- 0.65
100 micron	0.72 +/- 0.07	-1.47 +/- 0.88

[*] in the sense I(DIRBE)=Gain x I(IRAS) + Offset.

Reference 2

Session 57 – New Light on IRAS after DIRBE (COBE project presentation at the 185TH AAS Meeting)

Display presentation, Tuesday, January 10, 1995, 9:20am - 6:30pm

[57.07] New Light on IRAS After DIRBE

D.Leisawitz, et al.

The COBE Diffuse Infrared Background Experiment (DIRBE) and the Infrared Astronomical Satellite (IRAS) both surveyed the sky in broad photometric bands nominally at wavelengths of 12, 25, 60, and 100 micron. The products of these surveys are publicly available and are the foundations for a number of astronomical studies. It is thus important to understand these two similar photometric systems, particularly as the IRAS Sky Survey Atlas (ISSA) and other IRAS extended--emission data products are essential when spatial resolution better than the DIRBE's 42 X 42 arcminute field of view is needed.

This poster reports the results from a comparison of DIRBE and IRAS photometry. A major result, found by comparing the IRAS Zodiacal Observation History File scans to DIRBE observations made at matching solar elongation angles, is that the quoted intensities are well--described by an equation of the form I_nu(DIRBE) = G_nu I_nu(IRAS) + O_nu at all four wavelengths. Gain G_nu and offset O_nu parameters are presented, and practical advice is offered to researchers who may wish to apply a correction to the IRAS extended emission intensities.

The National Aeronautics and Space Administration/Goddard Space Flight Center (NASA/GSFC) is responsible for the design, development, and operation of the Cosmic Background Explorer (COBE). Scientific guidance is provided by the COBE Science Working Group. The COBE program is supported by the Astrophysics Division of NASA's Office of Space Science. The COBE and IRAS data products may be obtained from the NSSDC.

Reference 3

A Spitzer/SIRTF project note taken from Spitzer web page, http://ssc.spitzer.caltech.edu/documents/background/node3.html:

"The absolute brightness of the zodiacal light will be taken from a three-dimensional model of the distribution of interplanetary dust and its scattering and thermal emission. The model was normalized to the time-variation of the sky brightness observed by the Cosmic Background Explorer (COBE) Diffuse Infrared Background Experiment (DIRBE) in 1989-90. The absolute calibration of DIRBE is very secure, and its gain stability was sufficient to allow it to monitor the temporal variation of the sky brightness in each 0.7-degree beamwidth. The temporal variation of the brightness of a fixed celestial position was due to the changing viewing angle through the Solar System dust cloud, which it is a unique signature of the Zodiacal Light. The range of solar elongation (angle between the line of sight and the Sun) was 64-124 for DIRBE, which is essentially the same as that planned for SIRTF. Therefore, the DIRBE observations sample the essentially the same parts of the Solar System that SIRTF will. The wavelength coverage of DIRBE was 1.25-240 m, which spans the wavelength range of SIRTF. For comparison, the previous best estimator was the zodiacal light model fitted to the IRAS data (Good 1994). Differences between the COBE and IRAS zodiacal light models are certainly present, and they are largely attributed to the absolute calibration errors in the IRAS database. The IRAS absolute calibration for diffuse emission used offsets (as a function of time) forced to match a particular model of the zodiacal light brightness of the ecliptic pole. The actual sky brightness measured by COBE is different, and it has an annual variation with a different phase than the IRAS calibration model. The calibration differences are always less than 20%..."

Discussion

The question of the applicability of applying a recalibration for extended sources but not point sources translates from a spatial to a temporal one when considered at the detector

level. Consider the response of a single element IR detector to input radiation. In the static case, the response is determined by the convolution of the system response (L,w) * beam profile(L,X) * source surface brightness (L,X). For the ideal case of a "square" beam profile, the location of the source in the aperture is irrelevant, if the source is smaller than the aperture. For the typical non-ideal case, the beam profile has structure, especially at the edges of the field of view, a source has structure to it, and the actual signal depends on how the source flux maps onto the aperture.

In the non-static case, where the instrument is moving across a source, the beam profile scans across the target. How the object is scanned can affect the resulting signal quite a lot, unless the beam profile is simple and symmetric. Further, the effective on-source integration time can vary quite a lot depending on how long the object is in the filed of view. Finally, the frequency response of the detector can be important, for objects that are compact and bright compared to the mean background.

The COBE/DIRBE 10-band, single element photometer was designed to avoid the problems of asymmetric beam patterns and instrument gains variable with frequency. The former issue was addressed with an off-axis Cassegrain telescope design and a redundantly baffled foretube. The latter was addressed by using an internal cryogenic chopper running at 4 HZ to chop the sky signal vs. an internal cold stop held at 2.7 K (the on-board superfluid helium tank temperature). The spin rate of the spacecraft was 2 RPM, and the angle of offset of the DIRBE telescope from the spin axis was 30 degrees, so that the effective scan rate across the sky was ~1 RPM in a torus 0.7 degrees thick by 180 degrees wide. The detectors were sampled at 32 HZ, for 8 samples per chop cycle. Thus the effective response frequency was always set by the chopper, and the DIRBE point source calibration and extended source calibration, allowing for beam profile effects, were the same. Absolute calibration was provided by measuring the signals found for known point sources: Sirius from 1-12 micron, NGC 7027 for 25 micron, Uranus for 60 and 100 micron, and Jupiter at 160 and 240 micron. M Cohen et al. (1998) found good agreement between the DIRBE calibrations scheme and one based on ground based observations of IR bright standards:

"The absolute calibration of the COBE/DIRBE data in the range 1-25 micron is examined through the in-band fluxes of DIRBE's own set of point-source calibration objects. Using the values of DIRBE fluxes expected for Sirius and for 10 of our published set of absolutely calibrated K and M giants that are in common with DIRBE's own calibration network, I find consistency with the project's formal basis, namely, our published calibrated spectrum of Sirius. This consistency means that one can use the DIRBE radiometry to construct absolutely calibrated "stellar templates" (i.e., continuous calibrated spectra from 1 to 35 micron) on the assumption that the intrinsic stellar spectrum of a star of given spectral class matches the intrinsic spectrum for the star of the same spectral class among the set of K and M giants, the spectrum of which has been absolutely defined. This technique is validated using a set of early M giants with well-characterized ground-based photometry and confirmed with IRAS low-resolution spectra."

For the pioneering IRAS mission, the case was different. While IRAS did utilize cold MOSFET Trans-Impedance Amplifier (TIA) similar to the JFET TIAs used by COBE/DIRBE, there was no internal mechanism to define the detector frequency response to an input source like the DIRBE chopper. Lacking an internal chopper, the detector response time would be set by the manner in which the focal plane scanned across an image. Detector response typically decreases as the signal modulation frequency increases. This is the reason for the "DC survey rate response" calibration correction (page IV-9 of the IRAS Explanatory Supplement) applied by the IRAS science data pipeline to the data. A highly extended source would have lower response frequencies, implying detector response closer to the static ideal than a compact source. OTH, an extended source response will vary more strongly with the beam pattern. For detectors with strongly varying gains as a function of scan frequency, this may lead to fundamentally different outputs for the survey scans and pointed AO observations of a target. The effect can be as large as 30% in the IRAS detectors. Both effects need to be taken into account in order to understand the resulting data. With respect to the IRAS point source calibration, Cohen et al. (1992) found the following: "...Preliminary

indications are that the IRAS is too high by 2%, 6%, 3%, and 12% at 12, 25, 60, and 100 micron, respectively."

As Mark Sykes pointed out in the PDS telecon, the physical size of the IRAS detectors varied by band, but was on the order of 1 x 1'; the effective pixel size in the IRAS maps was approximately 1' in the along scan direction, and approximately 4' in the cross scan direction, due to the sparseness of overlaps between scans. While most of the comets observed by IRAS were point sources on this scale, some clearly were not, including Tempel 1. The point source detection algorithm described on page V-10 of the IRAS Explanatory Supplement returned values of the total flux for these comets that was too small, as the negative portions of the TOD filter subtracted coma from coma. This is the reason the Deep Impact project asked Russ Walker to re-extract the Tempel 1 comet data from the IRAS TOD stream, using a different filtering process. In the re-processed images of Walker (2000) and (2001), comet Tempel 1 varied from 6 to 20 re-constructed pixels FWHM, depending on wavelength and time of observation. While it is clear that Tempel 1 was extended to the IRAS pixellated detectors, it is not clear if the comet was large enough compared to an instantaneous detector FOV to expect the full gain variation due to varying effective scan frequency that requires the "DC survey rate response" correction. This is the reason for the statement in the Beichman and Wheelock IRAS project memo stating "…shows the IRAS measurements at 60 and 100~ micron were too bright relative to DIRBE at large spatial scales. There is no simple prescription for unraveling the varying spatial response of the detectors to effect a more accurate calibration for the ISSA images."

Suggestions for Future Work

A few actions could be taken to constrain this issue. First, compare the SED's found for the IRAS AO and Survey observations of Tempel 1 in 1983. The scan rates for the two sets of observations were very different, with the pointed AO observations scanning much more slowly. A difference in the extracted in-band fluxes should be found.
Second, the last line of the Beichman and Wheelock IRAS memo suggests another course

of action: "The data given in the table below, serve, however, to bound the problem to being no worse than a 28% effect at 100 micron, 13% at 60 micron, and 12% in a 60/100 micron color." Therefore, create model fits to the IRAS photometry which has had the DIRBE/IRAS correction applied, and for IRAS photometry which has had no correction applied. This will bound the problem, albeit possibly at the price of a large phase space of possible model solutions for the emitted dust.

VI References

Beichman, C.A., Neugebauer, G., Habing, H.J., Clegg, P.E., Chester, T., 1988, IRAS Catalogs and Atlases, Vol 1. Explanatory Supplement. Available online at http://www.ipac.caltech.edu.

Cohen, M., Walker, R.G., Witteborn, F.C., 1992, Spectral Irradiance Calibration in the Infrared., II – Alpha Tau and the Recalibration off the IRAS Low Resolution Spectrometer, AJ, 104, 2030 – 2044.

Cohen, M., 1998, Spectral Irradiance Calibration in the Infrared, IX - Calibrated Stellar Spectra Using DIRBE Radiometry, AJ, 115, 2092-2096.

Cohen, M., Walker, R.G., Barlow, M.J., Deacon, J.R., 1992, Spectral irradiance calibration in the infrared, I - Ground-based and IRAS broadband calibrations, AJ, 104, 1650-1657.

Leisawitz, D., Hauser, M. G.; Kelsall, T., Silverberg, R. F., Odegard, N., Stemwedel, S., Weiland, J., Burdick, S., Gautier, T. N., Gillett, F. C., Murdock, T. L., Neugebauer, G., Reach, W. T., Wheelock, S., 1994, New Light on IRAS After DIRBE, American Astronomical Society, 185th AAS Meeting, #57.07, Bulletin of the American Astronomical Society, Vol. 26, 1409.

Lisse, C.M., A'Hearn, M.F., Hauser, M.G., Kelsall, T., Lien, D.J., Moseley, S.H., Reach, W.T., Silverberg, R.F., 1998. Infrared Observations of Comets by COBE, ApJ. 496, 971 – 991.

Lisse, C. M., A'Hearn, M. F., Farnham, T. L., Groussin, O., Meech, K. J., Fink, U., Schleicher, D. G., 2005, The Coma of Comet 9P/Tempel 1, Space Science Reviews, Volume 117, Issue 1-2, pp. 161-192.

Lynch, D.K., Hackwell, J.A., Edelsohn, D., Lahuis, F., Roelfsema, P.R., Wesselius, P.R., Walker, R.G., Sykes, M.V., 1995, IRAS LRS Spectra of Comets Tempel 1 and Tempel 2, Icarus 114, 197 – 202.

Neugebauer, G., et. al. 1984, The Infrared Astronomical Satellite (IRAS) Mission, ApJ, 278, L1-L6.

Olnon, F.M., et. al., 1986. IRAS Catalogues and Atlases. Atlas of low-resolution spectra, A&A, 65, 607 – 1065.

Raimond, E.D., Beintema, D.A., Wesselius. P.R., 1985, In IRAS Catalogs and Atlases – Explanatory Supplement (C.A. Beichman *et al.*, Ed.), California Institute of Technology, Infrared Processing and Analysis Center (IPAC), Pasadena, CA.

Rieke, G.H., Thompson, R.I., Werner, M.W., Witteborn, F.C., Becklin, E.E., 1986. Infrared astronomy after IRAS, Science, 231, 807 – 814.

Sykes, M.V., Lien, D.J., Walker, R.G., 1990, The Tempel 2 Dust Trail, Icarus, 86, 236 – 247.

Sykes, M.V., Walker, R.G., 1992, Cometary Dust Trails I - Survey, Icarus, 95, 180-210.

Walker, R.G., Aumann, H.H., 1984, IRAS observations of cometary dust, Adv. Space Res. 4, No. 9, 197 – 201.

Walker, R.G., 1986a, IRAS Comets in Infrared Astronomical Satellite Asteroid and Comet Survey (D. Matson, Ed.), Infrared Processing and Analysis Center (IPAC), JPL D-3698, Ch. 3, 1-22.

Walker, R.G., Matson, D.L., Veeder, G.J., 1986b, IRAS observations of comets, Adv. Space Res. 6, No. 7, 57 – 66.

Walker, R.G., 2000, Explanatory Supplement to the 9P/Tempel 1 IRAS Survey Images Document in the NASA Planetary Data System Archives.

Walker, R.G., 2001, Explanatory Supplement to the IRAS Additional Observations of 9P/Tempel 1 Document in the NASA Planetary Data System Archives.

Young, E.T., 1982, Detectors in astronomy – Infrared astronomy, Nature 298, 796 – 798.

Online references:

http://www.ipac.caltech.edu/ipac/newsletters/oct93/cobe.html

http://ssc.spitzer.caltech.edu/documents/background/node3.html